

PRIMARY PRODUCTIVITY OF *SPARTINA ALTERNIFLORA* FOLLOWING FREEZE-INDUCED MANGROVE LOSS IN SOUTH TEXAS

Carole-Lynna Benhamou, The University of Texas at Austin
December 2023

Abstract

A mixed mangrove and marsh community in south Texas experienced a record freeze event in February 2021. The event resulted in the mortality of over 99% of the black mangrove, *Avicennia germinans*, which had previously dominated the vegetative community. With the loss of mangroves, the smooth cordgrass, *Spartina alterniflora* has rapidly expanded throughout the entire wetland. To document the changing post-freeze edaphic conditions and their effects on *S. alterniflora* photosynthetic performance, we collected data on various environmental and plant physiological parameters within the wetland habitat mosaic. We examined recolonizing *S. alterniflora* monocultures, two transitional patches containing both species, two healthy reference *S. alterniflora* patches, one live and one dead mangrove patch, and an unvegetated patch. Recolonizing *S. alterniflora* patches recorded higher redox potentials (180.040 ± 154.395 mV) than the dead mangrove patch (-394.239 ± 40.378 mV). We observed similar mean net photosynthetic rates for both the reference (2.486 ± 3.773 $\mu\text{mol CO}_2 \text{ m}^{-2} \text{ s}^{-1}$) and recolonizing (3.047 ± 3.721 $\mu\text{mol CO}_2 \text{ m}^{-2} \text{ s}^{-1}$) *S. alterniflora* patches. Based on these results, *S. alterniflora* has successfully overcome the low redox conditions that characterize this altered community, reaffirming its former dominance in this coastal wetland ecosystem. The change in vegetation dominance illustrates how *S. alterniflora* can adapt to the changing environmental conditions seen in south Texas.

Introduction

A mosaic of temperate salt marsh plants and tropical mangroves exist in coastal wetlands of temperate-tropical climate transition zones (Ross et al. 2009). The tropicalization of coastal wetlands in these climate transition zones has been observed because of winter climate change increasing winter temperatures (Osland et al. 2013). The US gulf coast is a climate transition zone and has witnessed the northward range expansion of black mangroves, *Avicennia germinans*, into temperate saltmarsh regions, which contain the smooth cordgrass, *Spartina alterniflora* (Cavanaugh et al. 2019). *A. germinans* has been able to establish dominance because they can also out shade *S. alterniflora* since mangroves have higher biomass and grow into trees (Stevens et al. 2006). The expansion of mangroves into marshes and the subsequent shift in community composition will likely have substantial impacts on ecosystem service provisions of the wetland (Osland et al. 2013).

Mangroves and salt marshes alike provide valuable, but different ecosystem services (Barbier 2007). The tall woody biomass of mangroves protects coastlines from storm surge damage and erosion by reducing the height, duration, and velocity of incoming waves (Barbier et al. 2011). The complex and dense root structures of mangroves enable sediment stabilization and encourage particle retention and deposition, all which help control erosion (Barbier et al. 2011). Mangrove root structure also provides suitable reproductive habitat and sheltered living space for offshore fisheries (Barbier et al. 2011). The tightly packed vegetation structure of marshes provides habitat that is mainly inaccessible to large predatory fish. This protection allows increased growth and survival of various ecologically and economically important marine species like oysters, shrimp, and juvenile fish (Boesch and Turner 1984). Upright salt marsh grasses slow water from rivers, terrestrial runoff, rain, and groundwater, and function as natural filters that facilitate

suspended sediment deposition from the water and nutrient uptake by salt marsh grasses (Morgan et al. 2009). Plant uptake of excess nutrients like nitrogen helps prevent the eutrophication of downstream ecosystems like bays, estuaries, and oceans (Jordan et al. 2011).

Mangroves and salt marshes are among the most productive ecosystems in the world (Alongi 2020). Salt marshes sequester more (24 %) net primary productivity than mangroves (12 %), but mangroves proportionally store more carbon (739 Mg C ha⁻¹) than salt marshes (334 Mg C ha⁻¹) (Alongi 2020). One of the main regulators of high primary productivity in these ecosystems is tidal energy, which indirectly allows plants to allocate more of their energy for growth and reproduction (Alongi 2020). High primary productivity indicates high rates of deposition of organic carbon into the sediment in the form of dead plant matter (Chmura et al. 2003). The dense vegetation and structural complexity of the root systems in mangrove and marsh ecosystems efficiently trap sediment sourced internally and externally, and its associated organic carbon (Chmura et al. 2003). In addition to deposition of organic carbon, tidal inundation reduces oxygen content in wetland sediments since diffusion rates of oxygen in water are slow. Anoxic sediment conditions slow microbial decomposition of organic carbon by limiting the availability of oxygen as the final electron acceptor in microbial aerobic respiration (EPA Office of Water Office of Science 2008). Microbes then use less efficient respiration pathways with alternative final electron acceptors. This slows the remineralization and decomposition of buried organic carbon in anoxic sediments, which allows for long term carbon burial in marsh and mangrove sediments, with mangroves storing twice as much organic carbon as marshes (Alongi 2020).

Because mangroves and salt marshes are ecologically valuable and function as global carbon sinks (Alongi 2020), it is important to understand how primary productivity may be impacted by shifts in community composition. As climate change continues, extreme weather

events such as freezes, will increase in magnitude and frequency (IPCC 2023). Winter storm Uri, a 14-day freeze event in 2021, caused the death of over 99% of *A. germinans* along the Texas coast. Preliminary observations indicate that the subsequent decomposition of mangrove plant biomass, including root and rhizome tissues, added organic carbon to estuarine soils and caused hypoxic conditions (Dunton, unpub data). *S. alterniflora* was able to persist through the event since it is more cold-tolerant than *A. germinans* (McKee 1993), and *S. alterniflora* tends to rapidly recolonize after winter freezes cause the dieback of *A. germinans* (Stevens et al. 2006) (Fig. 1). In the process, *S. alterniflora* removes available nutrients from the soil, which can cause root competition for nutrients between the grass and new mangrove seedlings (Patterson et al. 1993). *S. alterniflora* is an efficient user of available nutrients, which produces significant amounts of organic matter (Materne et al. 2022).



Figure 1: Image of *S. alterniflora* surrounded by dead mangroves. Photo taken in Port Aransas, TX, 2 years after winter storm Uri.

This study assesses *S. alterniflora* that is growing in former mangrove habitats. We compare soil and photosynthetic parameters of various vegetative composition throughout the wetland: *S. alterniflora* growing in pure stands, recolonizing *S. alterniflora* that is growing within vast areas of dead mangroves, transitional patches with both *S. alterniflora* and *A. germinans*, an

unvegetated patch, live, and dead *A. germinans* patches. We hypothesize that (1) post-freeze soil conditions in recolonizing *S. alterniflora* patches are characterized by high soil organic matter and low redox potentials, and that (2) patches of recolonizing *S. alterniflora* can withstand soils with low redox potentials; however, primary productivity is low. This study will increase our understanding of the performance of *S. alterniflora* in wetland soils following freeze-induced mangrove loss.

Materials and Methods

Study site

We conducted this study on Coyote Island, a portion of Mustang Island located in South Texas (Fig. 2), from June to August in 2023.

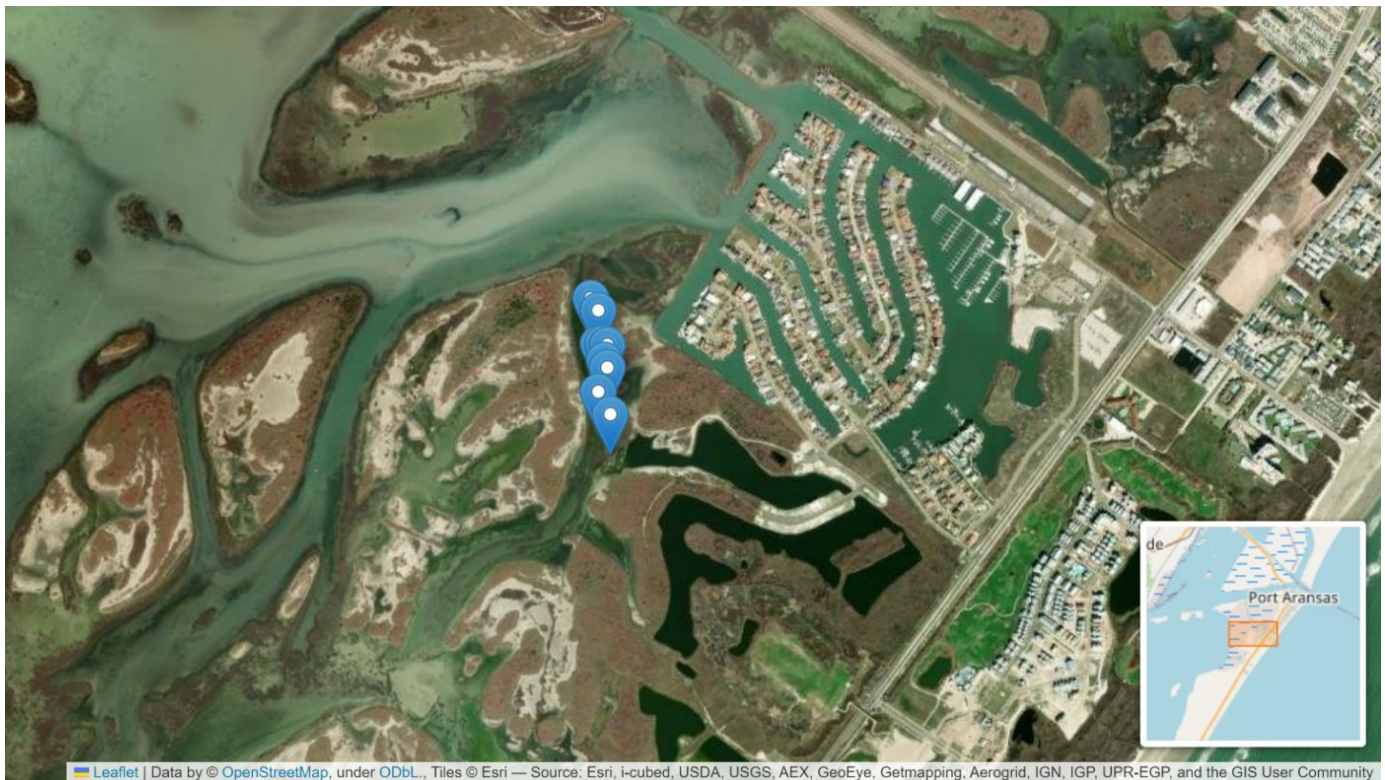


Figure 2. Locator map of the study site. Blue markers indicate the different patches.

Wetlands on Coyote Island consist of a saltmarsh – mangrove ecotone that were dominated by *A. germinans*.

Field methods

In May 2023, we identified four patches of interest: two patches of *S. alterniflora* growing within dead mangroves and two transitional patches with both *S. alterniflora* and live *A. germinans*. We also identified five reference patches: two healthy *S. alterniflora* patches not growing within dead mangroves, one live and one dead *A. germinans* patch, and one bare patch. The reference patches serve as end members of each vegetation type for us to contextualize the data from the first four patches with what is going on in the greater habitat (Fig. 3).

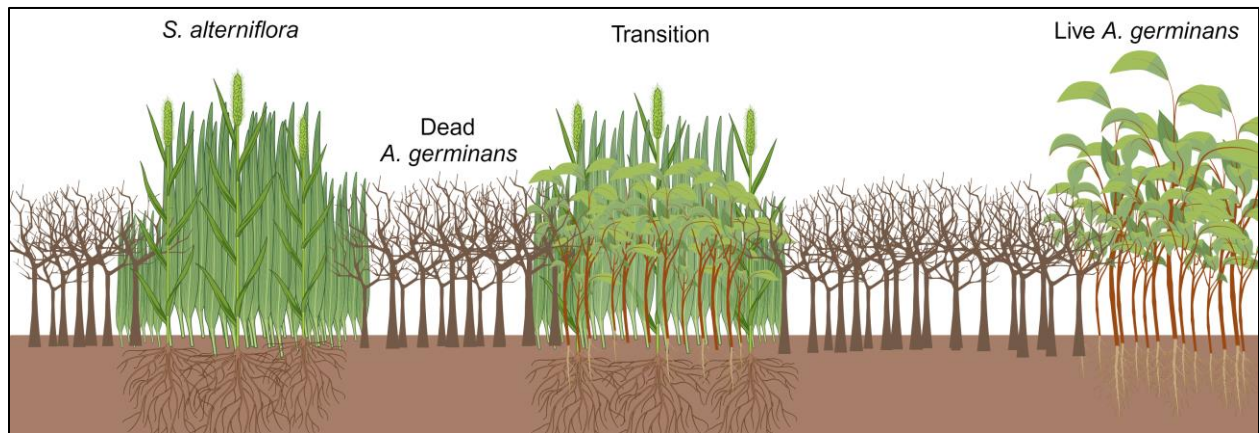


Figure 3. Schematic of the landscape mosaic on Coyote Island, not to scale (credit: biorender.com).

We demarcated patch extent using flags and measured the patch dimensions across the sets of flags. To assess the dominant cover type for each patch, we measured the percent cover of *S. alterniflora*, live and dead *A. germinans*, water, and mud. We collected other environmental data such as air and soil temperature, maximum canopy height, and water depth if any was present in the patch. We used the Mustang Beach airport weather station hotline to determine air temperature. We measured soil temperature using the Omega HH-25KC digital thermometer. Temperature controls many microbial mediated biogeochemical reactions in the sediment and water column, where higher temperatures increase microbial metabolism (Chmura et al. 2003). Water depth limits

the amount of oxygen able to diffuse from the air into the sediment and power microbial metabolism of organic carbon (EPA Office of Water Office of Science 2008).

To assess biogeochemical conditions, we collected three replicates of 30-cm soil cores for all patches and one 10-cm core at each patch to determine the distribution of sediment grain sizes. All cores were stored in WhirlPacs on ice to slow any microbial activity while in transit to the lab. We then froze the samples until lab processing.

To measure redox, we used a redox microelectrode (Unisense A/S) and 1-m long soil corers with holes drilled every cm. We covered the holes in at least two layers of packing tape to ensure the sediments were not exposed to oxygen. First, we calibrated the reference Ag/AgCl electrode (Unisense A/S) with the redox microelectrode calibration kit (Unisense A/S). We then pounded the core liner into the ground at each patch to an approximate depth of 32 cm, capped the top of the core, pulled the core out of the ground, and capped the bottom of the core. Then, we laid the core horizontally, and measured the total length of sediment collected. Starting at the top of the core, we took 5 to 7 redox measurements for every cm in the first 4 cm, then every 2 cm from a depth of 4 to 20 cm, then every 4 cm from a depth of 20 to 32 cm. We measured two cores from both recolonizing *S. alterniflora* patches, and one core for all other patches in the field.

The redox potential at any point in the sediment column gives insight to the oxidation state, and by extension whether microbes are conducting oxidative metabolism or not. A positive redox potential indicates oxygen is the primary electron acceptor in microbial metabolism. A negative redox potential indicates that microbes are utilizing alternative electron acceptors for less efficient anaerobic metabolism, thus decomposing organic carbon at a slower rate (Froelich et al., 1979).

We used an infra-red gas analyzer (IRGA) (LI-6400; LI-COR Biosciences, Inc.) to collect plant physiology data (e.g., photosynthesis, respiration, and transpiration rates) in five out of the

nine patches (both transition and recolonizing *S. alterniflora* patches and one of the reference *S. alterniflora* patches). Plant respiration is a process in which plants produce H₂O, CO₂, and energy for growth and maintenance of plant tissues. All three parameters provide insight into the growth rates of *S. alterniflora* and *A. germinans*. We measured five to seven *S. alterniflora* leaves in all five patches, and three live *A. germinans* leaves in each of the two transition patches between 9AM and 12PM. We collected data for the leaves at ambient light and in the dark. We haphazardly selected the plants to measure within a patch and used the second leaf. All measurements were corrected to leaf area. We also haphazardly collected three replicates of leaves from the five patches to calculate tissue C:N:P.

Lab methods

We quantified soil organic matter (SOM) by measuring percent loss on ignition (LOI), soil moisture, carbon and nitrogen content, and $\delta^{13}\text{C}$ and $\delta^{15}\text{N}$ stable isotopes according to the following lab protocols: “Sediment Organic Carbon” (Dunton and Jackson 2009) and “Preparing Soil and Sediment Samples for EA-IRMS” (Bristol 2020, adapted from Brodie et al. 2011). SOM is an indicator of soil quality and an important source of nitrogen and micronutrients required for plant growth and microbial activity (Bruland and Richardson 2006). Sediment carbon and nitrogen content gives us an idea of how much of the nutrients have been deposited. To measure sediment porewater ammonium in the 30 cm cores, we thawed each sample, and followed Parsons’ Determination of Ammonia protocol (Butler 1984). Ammonia is a nutrient taken up by plants and is a byproduct of microbial decomposition of organic carbon. Higher sediment ammonium levels indicate increased remineralization of organic carbon and/or decreased plant uptake (Zhu et al. 2010).

We measured *S. alterniflora* and *A. germinans* leaf tissue C:N:P ratios according to the following protocols in lab: “Stable Isotope Analysis: Protocol and Procedures” (Jackson, Garlough, Dunton) and “Tissue Phosphorus Content.” This allowed us to identify the relationship between nutrient availability and marsh community structure.

Data analysis

All patches were visually compared for redox potential, sediment ammonium, sediment C:N ratio, and LOI with boxplots. We also created a boxplot of net photosynthetic rate for *S. alterniflora*, transition, and reference *S. alterniflora* patches. We calculated the net photosynthetic rate by subtracting the respiration rate (PAR = 0) from the photosynthetic rate (PAR = ambient conditions). We used R software to create all boxplots.

We ran a generalized linear mixed model (GLMM), which is an extension of the linear mixed model framework. Using a GLMM is appropriate because we needed a way to account for subject-specific variations that are not explained by fixed effects, and a flexible framework that would allow for the inclusion of both fixed and random effects. This provides a more realistic representation of the underlying data generating process.

We used the lmer class from the lme4 package in R (version 4.2.1). In the model, we specified net productivity ($\mu\text{mol CO}_2 \text{ m}^{-2} \text{ s}^{-1}$) as the response variable, and indicated the following predictor variables: sediment $\delta^{13}\text{C}$ (‰), carbon content (%), sediment $\delta^{15}\text{N}$ (‰), nitrogen content (%), soil moisture (%), redox potential (mV), and SOM (%). We defined the grouping variable for random effects as patch type, so that each group represents a cluster of observations and the model accounts for variability within and between these groups.

A regression analysis shows us which parameters significantly impact net productivity, if any, while accounting for patch type. Using regression analysis as opposed to running several t-tests or ANOVAs helps reduce statistical biases since we are only running one test and not several.

Results

Figures and data are not reported for all parameters collected. Several of the parameters show relationships that have been well studied or do not add much more to the story, so we did not include those in the results and discussion section of this report.

Sediment organic matter

Recolonizing *S. alterniflora* patches have the maximum SOM value of 2.781 % (Fig. 4). Recolonizing *S. alterniflora* has the greatest SOM (2.231 ± 0.473 %) and reference *S. alterniflora* has the least SOM (0.479 ± 0.416 %) (Fig. 4). Transitional patches have a greater mean SOM (1.713 ± 0.442 %) and more variability than the live mangrove patch (1.508 ± 0.348 %) (Fig. 4). Dead mangrove (1.023 ± 0.168 %) has a greater mean SOM than the bare patch (0.766 ± 0.159 %), and both these values are greater than the reference *S. alterniflora* mean SOM (Fig. 4).

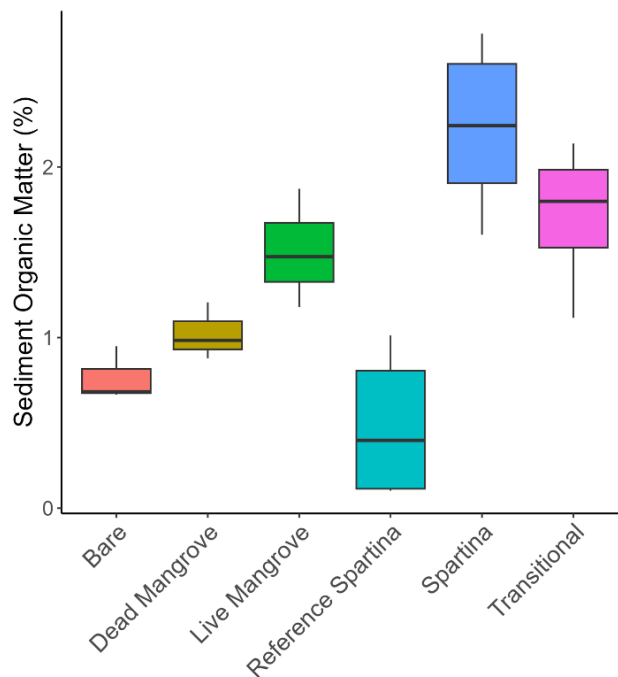


Figure 4. Boxplots of SOM content (%) for all patch types.

Sediment C:N ratio

The recolonizing *S. alterniflora* patches have C:N values from 9.917 to 11.871, which is slightly less than both the live and dead mangrove values (Fig. 5). Live mangrove soils have the highest mean C:N values (12.223 ± 0.736), and dead mangrove soils have very similar C:N values (12.173 ± 1.298) (Fig. 5). Reference *S. alterniflora* patches have one of the lowest mean C:N values (10.925 ± 0.811), and show the greatest variance amongst the patches (4.382 to 9.714) (Fig. 5). The upper part of the reference *S. alterniflora* boxplot overlaps with the mean and lower half of the bare patch's C:N values (9.670 ± 2.259) (Fig. 5).

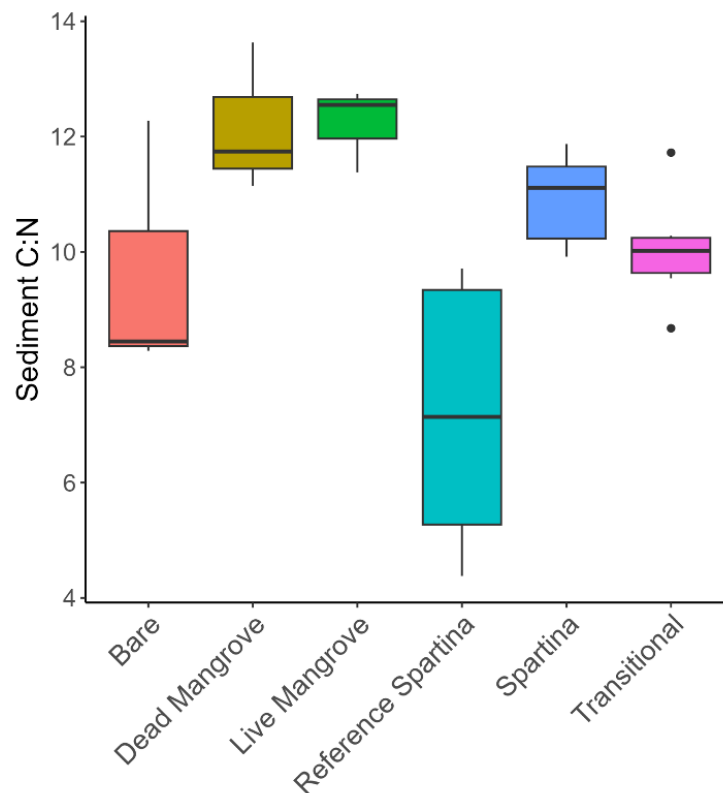


Figure 5. Boxplots of sediment carbon to nitrogen ratio for all patch types.

Sediment ammonium

Mean sediment ammonium levels are similar across all patch types except reference *S. alterniflora*, which has the highest mean and overall variance ($420.063 \pm 128.389 \mu\text{M}$) (Fig. 6). Recolonizing *S. alterniflora* patches have a greater mean ($146.816 \pm 72.982 \mu\text{M}$) than live

mangrove ($118.935 \pm 43.991 \mu\text{M}$), but less than that of dead mangrove ($159.218 \pm 71.702 \mu\text{M}$) (Fig. 6). Bare patch has the least variance of all patches and one of the lowest means ($97.000 \pm 22.434 \mu\text{M}$). Transitional patches have the lowest mean of all patches ($96.385 \pm 56.283 \mu\text{M}$) (Fig. 6).

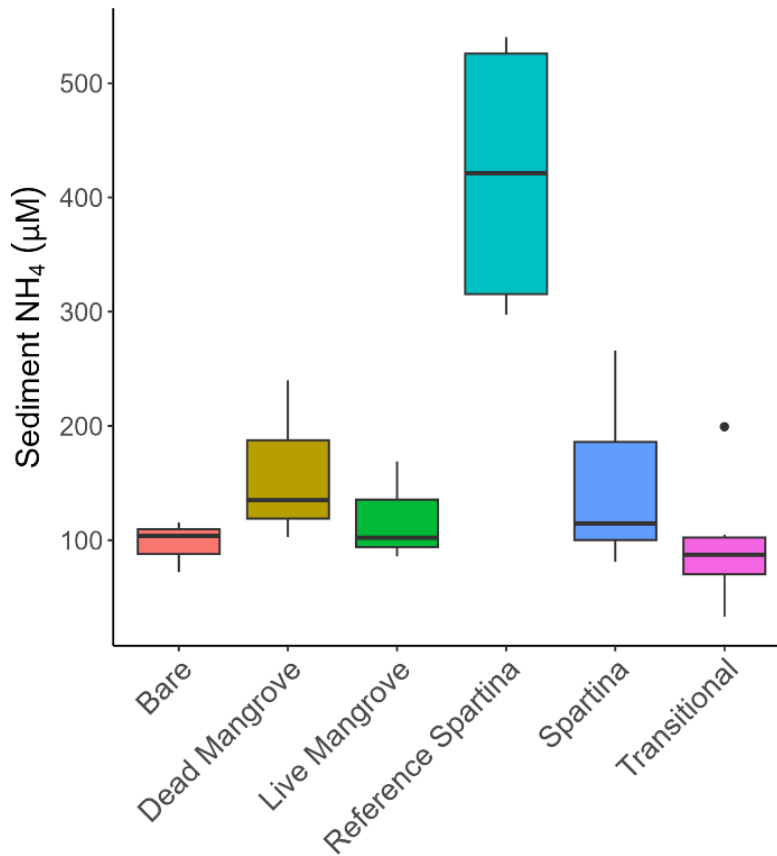


Figure 6. Boxplots of sediment ammonium (μM) for all patch types.

Redox potential

Reference *S. alterniflora* sediments have a greater mean redox potential ($-327.845 \pm 185.565 \text{ mV}$) than bare patch sediments ($-342.242 \pm 135.861 \text{ mV}$) (Fig. 7). Dead mangrove sediments have the lowest mean redox potential ($-394.239 \pm 40.378 \text{ mV}$), which is similar in value to reference *S. alterniflora* and the bare patch (Fig. 7). The recolonizing *S. alterniflora* patches have the highest redox potential ($180.040 \pm 154.395 \text{ mV}$) (Fig. 7). These values are similar to the

means for live mangrove (160.184 ± 212.936 mV) and transitional (-9.698 ± 175.405 mV) patches (Fig. 7).

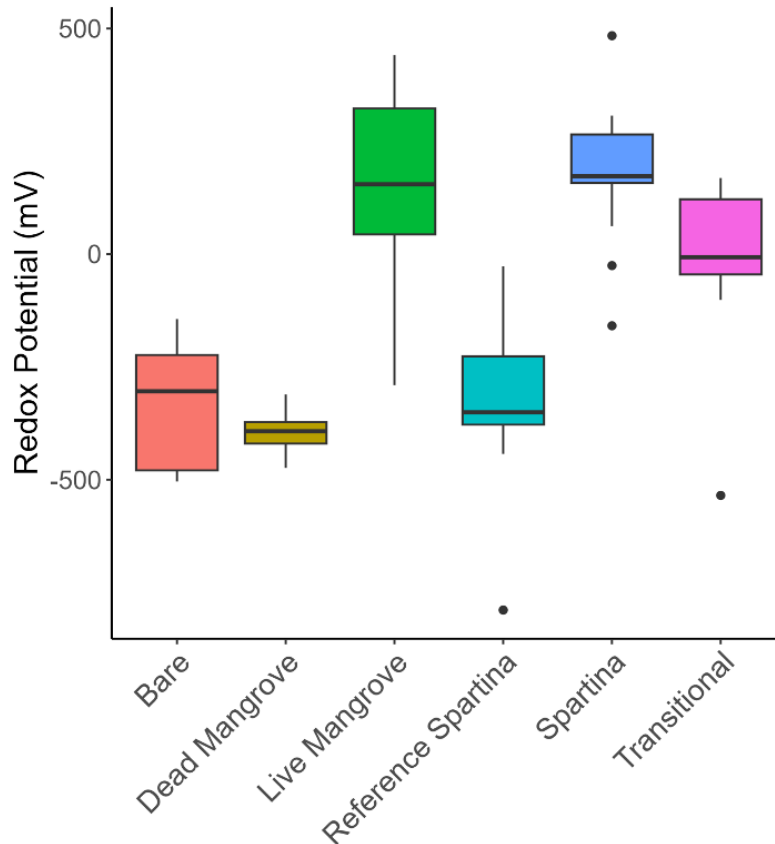


Figure 7. Boxplots of redox potential values (mV) across all patch types.

Net productivity data

There is a high amount of variability in the net photosynthetic rate for the recolonizing *S. alterniflora*, transitional, and reference *S. alterniflora* patches (figure 8). The reference *S. alterniflora* patch has the lowest mean net photosynthetic rate (2.486 ± 3.773 $\mu\text{mol CO}_2 \text{ m}^{-2} \text{ s}^{-1}$) when compared to the recolonizing *S. alterniflora* (3.047 ± 3.721 $\mu\text{mol CO}_2 \text{ m}^{-2} \text{ s}^{-1}$) and transitional (2.957 ± 2.851 $\mu\text{mol CO}_2 \text{ m}^{-2} \text{ s}^{-1}$) patches (figure 8). Though, overall, net photosynthetic rates of *S. alterniflora* are comparable across patch types (figure 8).

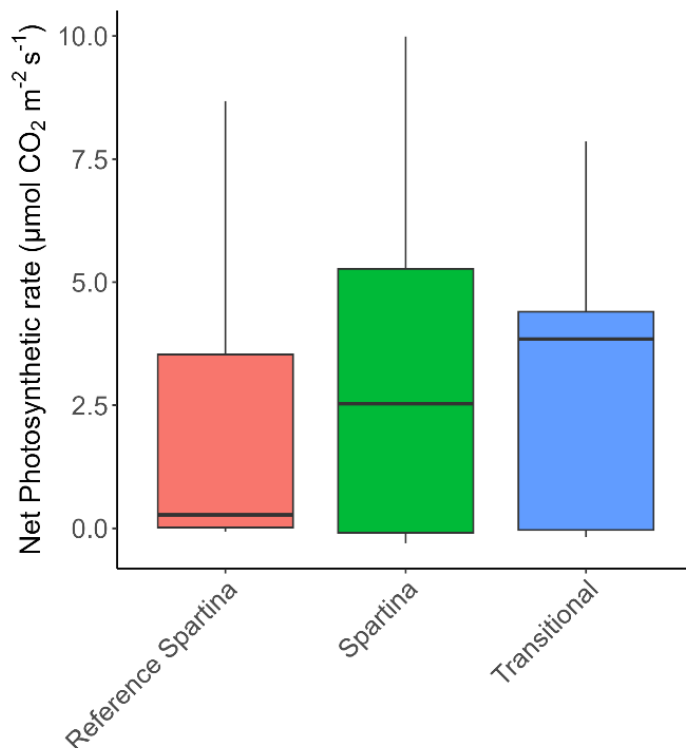


Figure 8. Boxplots of net photosynthetic rate ($\mu\text{mol CO}_2 \text{ m}^{-2} \text{ s}^{-1}$) of *S. alterniflora* across various patch types.

GLMM

None of the predictor variables (e.g., fixed effects) or random effect of patch type are statistically significant (table 1). The marginal R^2 is 0.3369 and the conditional R^2 is 0.6159.

Table 1. Summary of GLMM fixed effects results.

Fixed Effects	Estimate	Standard Error	df	t value	Pr(> t)
(Intercept)	19.73563	35.23662	0.78896	0.56	0.694
Sediment $\delta^{13}\text{C}$ (‰)	-0.28706	1.74059	0.88343	-0.165	0.899
Sediment C (%)	25.59121	18.58099	2.20416	1.377	0.292
Sediment $\delta^{15}\text{N}$ (‰)	-3.50128	2.24207	3.84387	-1.562	0.196
Sediment N (%)	-302.99424	192.11399	1.83016	-1.577	0.267
Soil moisture (%)	-0.69596	0.78244	3.9078	-0.889	0.425
Redox potential (mV)	-0.01203	0.01179	0.83017	-1.02	0.52
SOM (%)	3.72411	8.25208	3.39956	0.451	0.679

Discussion

Soil organic matter

High SOM values for recolonizing *S. alterniflora* indicate the presence of organic-rich sediments, as expected. Mangroves and grass-dominated salt marshes are known for having greater SOM values (Osland et al. 2018). The lack of vascular plants in dead mangrove and bare patches may explain why SOM is less than that observed in recolonizing *S. alterniflora*, transitional, and live mangrove patches (Osland et al. 2018). Dead mangrove and bare patches likely have a greater mean SOM than reference *S. alterniflora* because of the detrital organic matter input post-freeze. Furthermore, the reference *S. alterniflora* patches were located in either tidally flushed sediments or coarse-grained sandy sediments, possibly preventing the accumulation of SOM.

Sediment C:N ratio

Wetlands are sinks for organic carbon and nutrients (Schlesinger 1997; Mitsch and Gosselink 1993) and quickly begin to sequester these materials. Coastal wetlands tend to have sediment C:N ratios around 20:1 (Bianchi et al. 2013), but our sediment C:N ratios are less than this indicating a likely invasion of cyanobacteria. Once the mangroves died, there was not dense vegetation blocking sunlight, which may have allowed cyanobacterial invasion of dead mangrove sediment. An increase in cyanobacterial presence at the sediment surface could decrease the C:N ratio. This likely explains why the bare patches have the lowest C:N ratios. Dead mangrove, recolonizing *S. alterniflora*, and live mangrove sediments have similar C:N values that are greater than the bare patch because the organic matter inputs to the sediment come from plants with high C:N values (i.e., *S. alterniflora* and *A. germinans*). The reference *S. alterniflora* patches likely have the most variance because of their proximity to a tidal creek, thus indicating potential marine

organic matter sources such as phytoplankton which have low C:N relative to wetland plants (high C:N).

Sediment ammonium

Higher sediment ammonium indicates greater microbial decomposition since ammonium is a byproduct of microbial metabolism or reduced plant uptake (Sánchez-Pérez et al. 2021). The higher sediment ammonium values in the reference *S. alterniflora* and dead mangrove patches indicate more microbial decomposition of organic matter or reduced plant uptake.

Lower ammonium concentrations in the recolonizing *S. alterniflora* and transitional patches could be the result of higher plant uptake or higher amounts of microbial respiration, which can be a factor of oxygenated root zones or less organic matter (McKee et al. 2002). Nutrient uptake could be the main driver for lower ammonium concentrations since we sampled during *S. alterniflora*'s growing season, when nutrients such as ammonium are actively being taken up. Additionally, the lower ammonium concentrations could be a result of slowed microbial decomposition due to considerable amounts of refractory carbon compounds, such as lignin, and relatively lower nitrogen content in *S. alterniflora* litter (Perry and Mendelssohn 2009).

Redox potential

Redox potential is a measure of the oxidizing potential of sediments and directly impacts microbial respiration processes. Positive values indicate the presence of oxygen and an oxidizing environment. Negative values indicate a reducing environment.

Aerobic respiration dominates the near-surface, oxygenated sediments, and is the most efficient metabolic pathway for microbes (Froelich et al. 1979). However, anaerobic processes are

slower and less efficient, so anoxic sediment environments decrease the rate of organic matter remineralization and can promote long term carbon storage (Froelich et al. 1979).

The negative redox potentials for dead mangrove, reference *S. alterniflora*, and bare patches indicate anoxic conditions. The positive redox potentials for recolonizing *S. alterniflora*, transitional, and live mangrove patches indicate oxic conditions. However, the reference *S. alterniflora* patch is characterized as soils with low redox potentials.

We measured redox potential in late July to early August, when tides were low, so the patches were not regularly inundated with water. This likely exposed the sediment to oxygen more frequently (de la Cruz et al. 1989). Additionally, we sampled in the middle of the growing season, and *S. alterniflora* oxidizes the rhizosphere when photosynthesizing, which can create patches of oxygenated soils (de la Cruz et al. 1989). Sediment from bare and dead mangrove patches are expected to have negative redox potentials and be more anoxic because of the lack of live vegetation (de la Cruz et al. 1989).

Net productivity

The high amount of variability in the net photosynthetic rates across the vegetated patches is likely because we took measurements over a 3-hour period (9:00AM to 12PM), where the later measurements are closer to peak sunlight and the earlier measurements are within the early to late morning sun. At temperatures above 30°C, *S. alterniflora* has been shown to exhibit high photorespiratory activity and disabling of the C4 pathway (Shea 1977). The atmospheric temperature was at or greater than 30° C for all sample times (Wunderground 2023).

Net photosynthetic rates of *S. alterniflora* were similar across patch types indicating that *S. alterniflora* may not be impacted by changes in sediment biogeochemical conditions. The

reference *S. alterniflora* patch has a lower mean net photosynthetic rate compared to the recolonizing *S. alterniflora* and transitional patches, which may be explained by the negative redox potentials. Reducing soil conditions can cause root oxygen deficiencies and accumulation of toxic sulfides, which can impair growth (Mendelssohn and Morris 2000).

GLMM

The R^2 values of 0.3369 and 0.6159 indicate an overall poor fit of the model. When considering random effects (e.g., patch type), the R^2 almost doubles. While this is not necessarily an overall great fit of the predictor variables to net productivity, it accounts for about twice as much of the variance seen in the model. Both R^2 values are relatively low, which indicates that more samples or predictor variables likely need to be added to the model to explain the variance between net productivity and the predictor variables. This would likely improve the R^2 value and show an overall better fit of the model. In addition, the relatively low explained variance of the model supports our observation that net photosynthesis rates in *S. alterniflora* are not impacted by sediment biogeochemical conditions, and that other factors may be at play.

Concluding statements

Dead mangrove soils have low redox potentials and high sediment C:N values, which indicate anoxic conditions and refractory organic matter. Recolonizing *S. alterniflora* has high redox potentials, SOM, and sediment C:N values, which indicates oxic conditions and organic-rich sediments. While redox potential is high, which would favor high rates of microbial respiration, SOM and C:N also remain high, potentially indicating high organic matter inputs and reduced decomposition rates. Despite high soil variability, *S. alterniflora* maintains a consistent

rate of net photosynthesis, indicating resilience to changing abiotic conditions, further allowing *S. alterniflora* to recolonize wetland habitats following freeze-induced mangrove mortality (Martinez et al. 2023).

To further our understanding of *S. alterniflora* recolonization, the next steps of this project would include increasing the sample size, temporal extent, and breadth of variables measured. Collecting photosynthetic data over the entire course of the growing season, April to October, and sampling in a smaller window of time, so the photoinhibition effect is minimized in the data (Mo et al. 2023), will paint a better picture of the productivity of *S. alterniflora*. Increasing overall sample size would improve statistical accuracy and help account for the hyper-specific heterogeneity within the wetland mosaic. This would allow for data to be more easily compared to other locations. Additionally, collecting high precision elevation and sulfide data would likely improve model performance. Water inundation is a major limiting factor for wetland vegetation. Sulfate reduction to sulfide by anaerobic microorganisms is a common occurrence in marine sediment (Jørgensen et al. 2019), and sulfide data is easier to interpret than redox potential since the signal from a single electron acceptor is measured.

This study was a step forward in better understanding primary productivity of *S. alterniflora* in a formerly black mangrove dominated wetland post-freeze. Severe weather events are predicted to increase in magnitude and severity because of anthropogenic-induced climate change (IPCC 2023). As more severe weather events like freezes become more common, it is important to understand the implications of shifting vegetation populations since this can impact the carbon sink function of wetlands.

Literature Cited

Alongi, D. M. 2020. Carbon Balance in Salt Marsh and Mangrove Ecosystems: A Global Synthesis. *Journal of Marine Science and Engineering* 8:767.

- Barbier, E. B. 2007. Valuing Ecosystem Services as Productive Inputs. *Economic Policy* 22:177–229.
- Barbier, E. B., S. D. Hacker, C. Kennedy, E. W. Koch, A. C. Stier, and B. R. Silliman. 2011. The value of estuarine and coastal ecosystem services. *Ecological Monographs* 81:169–193.
- Bianchi, T. S., M. A. Allison, J. Zhao, X. Li, R. S. Comeaux, R. A. Feagin, and R. W. Kulawardhana. 2013. Historical reconstruction of mangrove expansion in the Gulf of Mexico: Linking climate change with carbon sequestration in coastal wetlands. *Estuarine, Coastal and Shelf Science* 119:7–16.
- Boesch, D. F., and R. E. Turner. 1984. Dependence of fishery species on salt marshes: The role of food and refuge. *Estuaries* 7:460–468.
- Bolker, B. M. 2015. Linear and generalized linear mixed models. Pages 309–333 in G. A. Fox, S. Negrete-Yankelevich, and V. J. Sosa, editors. *Ecological Statistics*. First edition. Oxford University Press. Oxford.
- Brodie, C.R., M.J. Leng, J.S.L Casford, C.P. Kendrick, J.M. Lloyd, Z. Yongqiang, and M.I. Bird. 2011. Evidence for bias in C and N concentrations and $\delta^{13}\text{C}$ composition of terrestrial and aquatic organic materials due to pre-analysis acid preparation methods. *Chemical Geology* 282:67-83.
- Bruland, G. L., and C. J. Richardson. 2006. Comparison of Soil Organic Matter in Created, Restored and Paired Natural Wetlands in North Carolina. *Wetlands Ecology and Management* 14:245–251.
- Butler, E. I. 1984. A manual of chemical and biological methods for sea water analysis. *Deep Sea Research Part A. Oceanographic Research Papers* 31:1523.
- Calvin, K., D. Dasgupta, G. Krinner, A. Mukherji, P. W. Thorne, C. Trisos, J. Romero, P. Aldunce, K. Barrett, G. Blanco, W. W. L. Cheung, S. Connors, F. Denton, A. Diongue-Niang, D. Dodman, M. Garschagen, O. Geden, B. Hayward, C. Jones, F. Jotzo, T. Krug, R. Lasco, Y.-Y. Lee, V. Masson-Delmotte, M. Meinshausen, K. Mintenbeck, A. Mokssit, F. E. L. Otto, M. Pathak, A. Pirani, E. Poloczanska, H.-O. Pörtner, A. Revi, D. C. Roberts, J. Roy, A. C. Ruane, J. Skea, P. R. Shukla, R. Slade, A. Slangen, Y. Sokona, A. A. Sörensson, M. Tignor, D. Van Vuuren, Y.-M. Wei, H. Winkler, P. Zhai, Z. Zommers, J.-C. Hourcade, F. X. Johnson, S. Pachauri, N. P. Simpson, C. Singh, A. Thomas, E. Totin, P. Arias, M. Bustamante, I. Elgizouli, G. Flato, M. Howden, C. Méndez-Vallejo, J. J. Pereira, R. Pichs-Madruga, S. K. Rose, Y. Saheb, R. Sánchez Rodríguez, D. Ürge-Vorsatz, C. Xiao, N. Yassaa, A. Alegría, K. Armour, B. Bednar-Friedl, K. Blok, G. Cissé, F. Dentener, S. Eriksen, E. Fischer, G. Garner, C. Guivarch, M. Haasnoot, G. Hansen, M. Hauser, E. Hawkins, T. Hermans, R. Kopp, N. Leprince-Ringuet, J. Lewis, D. Ley, C. Ludden, L. Niamir, Z. Nicholls, S. Some, S. Szopa, B. Trewin, K.-I. Van Der Wijst, G. Winter, M. Witting, A. Birt, M. Ha, J. Romero, J. Kim, E. F. Haites, Y. Jung, R. Stavins, A. Birt, M. Ha, D. J. A. Orendain, L. Ignon, S. Park, Y. Park, A. Reisinger, D. Cammaramo, A. Fischlin, J. S. Fuglestvedt, G. Hansen, C. Ludden, V. Masson-Delmotte, J. B. R. Matthews, K. Mintenbeck, A. Pirani, E. Poloczanska, N. Leprince-Ringuet, and C. Péan. 2023. IPCC, 2023: Climate Change 2023: Synthesis Report. Contribution of Working Groups I, II and III to the Sixth Assessment Report of the Intergovernmental Panel on Climate Change [Core Writing

Team, H. Lee and J. Romero (eds.)]. IPCC, Geneva, Switzerland. First. Intergovernmental Panel on Climate Change (IPCC).

Cavanaugh, K. C., E. M. Dangremond, C. L. Doughty, A. P. Williams, J. D. Parker, M. A. Hayes, W. Rodriguez, and I. C. Feller. 2019. Climate-driven regime shifts in a mangrove-salt marsh ecotone over the past 250 years. *Proceedings of the National Academy of Sciences of the United States of America* 116:21602–21608.

Chmura, G. L., S. C. Anisfeld, D. R. Cahoon, and J. C. Lynch. 2003. Global carbon sequestration in tidal, saline wetland soils. *Global Biogeochemical Cycles* 17.

de la Cruz, A. A., C. T. Hackney, and N. Bhardwaj. 1989. Temporal and spatial patterns of redox potential (Eh) in three tidal marsh communities. *Wetlands* 9:181–190.

EPA Office of Water Office of Science, U. 2008. Methods for evaluating Wetland Condition #18 Biogeochemical Indicators.

Froelich, P. N., G. P. Klinkhammer, M. L. Bender, N. A. Luedtke, G. R. Heath, D. Cullen, P. Dauphin, D. Hammond, B. Hartman, and V. Maynard. 1979. Early oxidation of organic matter in pelagic sediments of the eastern equatorial Atlantic: suboxic diagenesis. *Geochimica et Cosmochimica Acta* 43:1075–1090.

Jordan, S., J. Stoffer, and J. Nestlerode. 2011. Wetlands as Sinks for Reactive Nitrogen at Continental and Global Scales: A Meta-Analysis. *Ecosystems* 14:144–155.

Jørgensen, B. B., A. J. Findlay, and A. Pellerin. 2019. The Biogeochemical Sulfur Cycle of Marine Sediments. *Frontiers in Microbiology* 10.

Martinez, M., M. J. Osland, J. B. Grace, N. M. Enwright, C. L. Stagg, S. Kaalstad, G. H. Anderson, A. R. Armitage, J. Cebrian, K. L. Cummins, R. H. Day, D. J. Devlin, K. H. Dunton, L. C. Feher, A. Fierro-Cabo, E. A. Flores, A. S. From, A. R. Hughes, D. A. Kaplan, A. K. Langston, C. Miller, C. E. Proffitt, N. G. F. Reaver, C. R. Sanspree, C. M. Snyder, A. P. Stetter, K. M. Swanson, J. E. Thompson, and C. Zamora-Tovar. 2023. Integrating Remote Sensing with Ground-based Observations to Quantify the Effects of an Extreme Freeze Event on Black Mangroves (*Avicennia germinans*) at the Landscape Scale. *Ecosystems*.

Materne, M., Bush, T., Houck, M., and S. Snell. 2022. Plant guide for smooth cordgrass (*Spartina alterniflora*). USDA-Natural Resources Conservation Service, Louisiana State Office. Baton Rouge, LA.

McKee, K. L. 1993. Soil Physicochemical Patterns and Mangrove Species Distribution--Reciprocal Effects? *Journal of Ecology* 81:477–487.

McKee, K. L., D. R. Cahoon, and I. C. Feller. 2007. Caribbean mangroves adjust to rising sea level through biotic controls on change in soil elevation. *Global Ecology and Biogeography* 16:545–556.

- McKee, K. L., I. C. Feller, M. Popp, and W. Wanek. 2002. MANGROVE ISOTOPIC ($\delta^{15}\text{N}$ AND $\delta^{13}\text{C}$) FRACTIONATION ACROSS A NITROGEN VS. PHOSPHORUS LIMITATION GRADIENT. *Ecology* 83:1065–1075.
- Mendelssohn, I. A., and J. T. Morris. 2000. Eco-Physiological Controls on the Productivity of *Spartina Alterniflora* Loisel. Pages 59–80 in M. P. Weinstein and D. A. Kreeger, editors. *Concepts and Controversies in Tidal Marsh Ecology*. Springer Netherlands, Dordrecht.
- Mitsch, W. J., and J. G. Gosselink. 2007. *Wetlands*. Wiley, Hoboken, NJ.
- Mo, X., Z. Zhang, Y. Li, X. Chen, S. Zhou, J. Liu, B. Wu, S. Chen, and M. Zhang. 2023. Inhibition of *Spartina alterniflora* growth alters soil bacteria and their regulation of carbon metabolism. *Environmental Research* 236:116771.
- Morgan, P. A., D. M. Burdick, and F. T. Short. 2009. The Functions and Values of Fringing Salt Marshes in Northern New England, USA. *Estuaries and Coasts* 32:483–495.
- Nakagawa, S., and H. Schielzeth. 2012. A general and simple method for obtaining r^2 from generalized linear mixed-effects models. *Methods in Ecology and Evolution* 4:133–142.
- Osland, M. J., N. Enwright, R. H. Day, and T. W. Doyle. 2013. Winter climate change and coastal wetland foundation species: salt marshes vs. mangrove forests in the southeastern United States. *Global Change Biology* 19:1482–1494.
- Osland, M. J., C. A. Gabler, J. B. Grace, R. H. Day, M. L. McCoy, J. L. McLeod, A. S. From, N. M. Enwright, L. C. Feher, C. L. Stagg, and S. B. Hartley. 2018. Climate and plant controls on soil organic matter in coastal wetlands. *Global Change Biology* 24:5361–5379.
- Patterson, C. S., I. A. Mendelssohn, and E. M. Swenson. 1993. Growth and Survival of *Avicennia germinans* Seedlings in a Mangal/Salt Marsh Community in Louisiana, U.S.A. *Journal of Coastal Research* 9:801–810.
- Perry, C. L., and I. A. Mendelssohn. 2009. Ecosystem effects of expanding populations of *Avicennia germinans* in a Louisiana salt marsh. *Wetlands* 29:396-406.
- Port Aransas, TX Weather historystar_ratehome. (2023). <https://www.wunderground.com/history/daily/us/tx/port-aransas/KRAS/date/2023-6-27>.
- Ross, M., P. Ruiz, J. Sah, and E. Hanan. 2009. Chilling damage in a changing climate in coastal landscapes of the subtropical zone: A case study from south Florida. *Global Change Biology* 15:1817–1832.
- Sánchez-Pérez, J. M., C. Martínez-Espinosa, S. Sauvage, A. B. Ahmad, P. A. Green, C. J. Vörösmarty, and J.-M. Sanchez-Perez. 2021. Denitrification in wetlands: A review towards a quantification at global scale. *Science of the Total Environment* 754:142398.
- Schlesinger, W. H. 1997. *Biogeochemistry an analysis of global change*. Academic Press, San Diego, CA.

- SHEA, M. L. 1977. Photosynthesis and Photorespiration in Relation to the Phenotypic Forms of *Spartina Alterniflora*. Ph.D., Yale University, United States -- Connecticut.
- Stevens, P. W., S. L. Fox, and C. L. Montague. 2006. The interplay between mangroves and saltmarshes at the transition between temperate and subtropical climate in Florida. *Wetlands Ecology and Management* 14:435–444.
- Zhu, Z., D. Dye, S. Faulkner, W. Forney, R. Gleason, T. Hawbaker, J. Liu, S. Liu, S. Prisley, B. Reed, M. Reeves, M. Rollins, B. Sleeter, T. Sohl, S. Stackpoole, R. Striegl, A. Wein, and Z. Zhu. 2010. Public Review Draft: A Method for Assessing Carbon Stocks, Carbon Sequestration, and Greenhouse-Gas Fluxes in Ecosystems of the United States Under Present Conditions and Future Scenarios.